IEEE Access
Multidisciplinary ⋮ Rapid Review ⋮ Open Access Journal

Received October 22, 2021, accepted December 1, 2021, date of publication December 10, 2021,
date of current version December 21, 2021.

Digital Object Identifier 10.1109/ACCESS.2021.3134558

An Incremental Quantity Based Distance Protection With Capacitor Voltage Estimation for Series Compensated Transmission Lines

MD. TANBHIR HOQ[1], JIANPING WANG[2], (Senior Member, IEEE), AND NATHANIEL TAYLOR[1]
[1]KTH Royal Institute of Technology, 100 44 Stockholm, Sweden
[2]Hitachi Energy, 722 26 Västerås, Sweden

Corresponding author: Md. Tanbhir Hoq (hoq@kth.se)

This work was supported in part by the Swedish Energy Agency through Swedish Centre for Smart Grids and Energy Storage (SweGRIDS), in part by Hitachi Energy, and in part by the Swedish Transmission Network Operator Svenska kraftnät.

ABSTRACT Series capacitors increase the power transfer limit of transmission lines. However, the protection of series compensated lines using only local measurement is challenging. Phasor based distance protection experiences delay and directional problems in the presence of a series capacitor. This paper presents an incremental quantity based distance protection algorithm for series compensated lines. The algorithm uses instantaneous voltage and current measurements from the local bus. It consists of capacitor voltage estimation, fault detection, phase selection, directional discrimination and distance estimation. The algorithm is extensively tested based on simulations with a line-end series capacitor, considering different source impedance ratios, fault inception angle, compensation levels, and fault resistance, location and type. This time-domain method is shown to work well, with fast decision time.

INDEX TERMS Series compensation, incremental quantity, capacitor voltage estimation, distance protection.

I. INTRODUCTION

Series capacitors are used in transmission lines to compensate for series inductive reactance and thereby to increase the power transfer capacity [1]. They provide a low-cost alternative to building new transmission lines [1]. However, the introduction of series capacitors creates problems for line protection, especially with higher levels of compensation [2], [3]. Distance protection is used extensively in transmission systems. Series capacitors reduce the security and reliability of distance protection and create delays in relay operation [4]. Differential protection is also used in series compensated lines, but the need for fast reliable communication between the line terminals creates some challenges as transmission lines are usually long. Moreover, high levels of series compensation can also cause reliability problems to differential relays [5], [6]. For these reasons, the protection of series compensated lines has been a challenge in the past few decades, especially with methods that can work with local measurements alone.

The associate editor coordinating the review of this manuscript and approving it for publication was Zhigang Liu.

A. CHALLENGES IN THE PROTECTION OF SERIES COMPENSATED LINES

Phasor based distance protection is widely used for the protection of transmission lines. A major point in favor of distance protection is its ability to operate with local measurement without the need for fast reliable communication channels between the line terminals. However, in the presence of a series capacitor, the reliability and security of phasor based distance protection are severely affected, especially with higher levels of series compensation. There are three main phenomena that hamper the operation of distance relays, namely:

- Voltage inversion
- Current inversion
- Sub-synchronous oscillation

Voltage and current inversion refer to the sudden changes in the phase angle of the measured voltage and current phasors upon a fault. These can lead to directional discrimination problems and delay in relay operation. The oscillation condition refers to the oscillation in the calculated impedance from voltage and current signals, which can lead to a delay in relay operation.

There has been a lot of work in the past few decades on mitigating these issues in traditional distance protection,

focused on the frequency domain [7], [8]. One approach was to estimate the voltage across the MOV and capacitor during a fault, based on modeling. An empirical method was proposed in [9], [10] for calculating the equivalent resistance and reactance of a capacitor bank. An analytical method was presented in [11], [12] for calculating the voltage across the capacitor bank. Other works compared different models of MOV characteristics for suitability in fault studies [13]. The next approach found in the literature is improvement of phasor estimation. In [14] both Fourier and differential equation-based estimation methods were compared for faults in series compensated lines. In [15] some other phasor estimation methods were compared including digital mimic filter, modified cosine, DC offset removal, cascade filter algorithm for phasor estimation in series compensated lines. The third category of work involves the implementation of adaptive distance protection. References [16]–[18] present some of the important works in adaptive distance relay setting for series compensated lines. In commercial relays, memory voltage polarization is used to counter voltage inversion, but solutions for current inversion are less common [19]. Sub-synchronous oscillation is usually dealt with by filters and adaptive relay characteristics [19].

Frequency domain protection usually has an inherent delay due to the calculation of phasor quantities from the measured instantaneous values. Additional delays are incurred in the presence of a series capacitor. Therefore, with increasingly tight requirements on the fault clearing time in transmission systems, the protection of series compensated lines may tend to faster time-domain based methods. Time-domain based protection methods are usually based on travelling waves or incremental quantities. They do not suffer severely from the voltage and current inversion and oscillation problems observed in the phasor domain. In this paper, a time-domain distance protection method is proposed for series compensated transmission lines. The method is based on incremental quantities and estimation of instantaneous voltage across the series capacitor.

B. INCREMENTAL QUANTITY PROTECTION

The use of incremental quantities is based on a current or a voltage in a faulted network being represented as the sum of its pre-fault value and an incremental value (or 'delta') caused by the fault. Protection relays can measure the incremental quantities by taking the difference between the present instantaneous value and the corresponding point in an earlier ac period.

A general expression can be written as in Equation 1, where $V(t)$ and $I(t)$ are the measured instantaneous voltage and current, ΔV and ΔI are the instantaneous incremental voltage and current, T is the period of the measured voltage or current, and n is the number of periods back in time that the pre-fault values are taken.

$$\begin{aligned} \Delta V &= V(t) - V(t - nT) \\ \Delta I &= I(t) - I(t - nT) \end{aligned} \tag{1}$$

The calculated incremental quantities last only for n cycles, because after n cycles the calculation window starts to include fault values. Analysis of incremental quantities is simple in a linear system with fixed sources, as the network can be modelled as impedances driven by the incremental voltage at the fault point. This has been an adequate approximation in traditional power systems at short timescales around the occurrence of a fault. In the presence of significant in-feed from power-electronic converters, the situation may deviate significantly from the assumptions. This is a general weakness of algorithms based on superposition, such as incremental quantities and symmetric components [20]. Even traditional synchronous generator sources impose a limit of some tens of milliseconds on incremental quantity methods, by how long these sources remain stationary after a fault [21].

The incremental quantity principle has been applied to transmission line protection in various ways [21]–[25]. These cover methods for fault detection, directional discrimination and distance estimation for transmission line faults, based on incremental quantities. Application of the incremental quantity principle becomes challenging in series compensated lines [23]. The most important issue for implementing incremental quantity protection in series compensated lines is to estimate the instantaneous voltage across the series capacitor, both before and during a fault. As incremental quantity protection works with instantaneous voltage and current values, the capacitor voltage estimation should be done without any delay.

This paper proposes a method to estimate the voltage across the series capacitor for implementing incremental quantity protection in series compensated lines. Distance estimation and directional discrimination based on incremental quantities are demonstrated. First, the proposed incremental solution is described, in section II. Then the test systems and different tested cases are described in section III, and the results are presented and discussed in section IV.

II. METHOD

The incremental voltages and currents are calculated by equation 1, using a delay of one period, $n = 1$. The incremental quantities are calculated for all three phases and for phase-to-phase where necessary. These cases are denoted by subscripts for phases a, b and c: for example ΔI_b for the incremental current in phase b, or ΔV_{ca} for incremental voltage between phases c and a.

The general structure of the proposed method is shown in figure 1. The capacitor voltage is calculated continuously using instantaneous current values. Upon fault detection, phase selection is done to select the fault loop. Information from the fault loop is then used to find the fault direction. Finally, the distance estimation is completed with information from the fault loop and capacitor voltage.

In the following subsections, each of these steps is explained. Simulation results are presented wherever necessary to explain the process. All simulations here are done in PSCAD [26]. A simplified model of the system that was

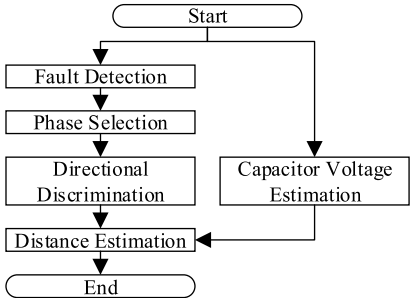

FIGURE 1. Schematic of the proposed method.

simulated in PSCAD is shown in figure 2. The model is of a 500 kV transmission line 200 km long. The series capacitor is located at one end of the line.

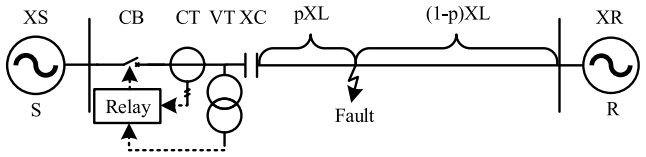

FIGURE 2. Simplified model of series compensated transmission line.

A. CAPACITOR VOLTAGE ESTIMATION

Estimating the voltage across the series capacitor has been one of the challenges in the protection of series compensated lines. A series capacitor is accompanied by overvoltage protection that will provide a shunt path during faults in which the capacitor voltage goes far above its normal operating level. Figure 3 shows a common configuration of a series capacitor bank, where the capacitor, a metal oxide varistor (MOV) and a bypass circuit breaker (CB) are all connected in parallel. The non-linear nature of the MOV makes the capacitor voltage estimation more challenging. During a fault the MOV starts conducting to limit the capacitor voltage to a pre-set protective threshold, usually around 2 to 3 times the capacitor's rated operation voltage. The bypass CB is closed to take the capacitor and MOV out of the fault loop when the MOV reaches its energy absorption threshold. Closing the bypass CB takes at least one ac period even for the highest fault currents in suitable conditions. For an algorithm that gives a decision in the first cycle after fault inception, the capacitor and MOV are therefore the only parts of figure 3 that need to be considered.

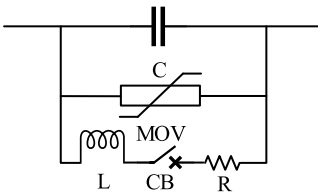

FIGURE 3. Capacitor bank protection.

The current-voltage relationship of a MOV is shown in figure 4 *a*. From this figure, the resistance-voltage characteristic of the MOV can be calculated as shown in 4 *b*. The resistance-voltage curve is shown with a fourth-order polynomial curve fitting. This will be used to interpolate resistance values for different voltages.

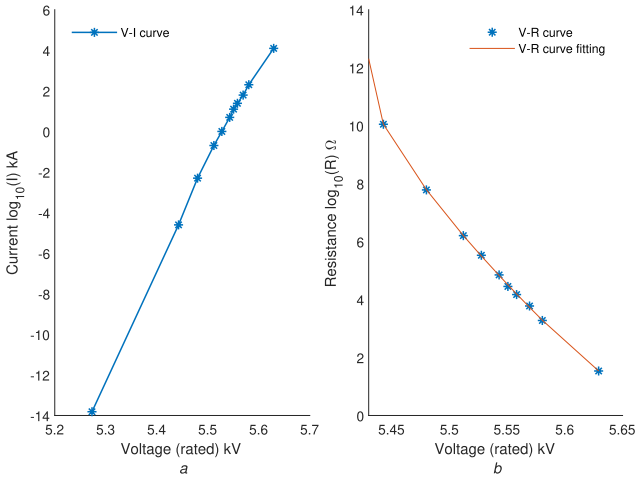

FIGURE 4. Characteristic curve of MOV a) V-I curve b) V-R curve.

The method for calculating the capacitor voltage is shown in figure 5. The capacitor voltage must continuously be estimated, to have pre-fault values available for calculation of the incremental voltage value during a fault. During testing with simulation data the first sample of estimated capacitor voltage (V_c) was initialized during the first period by multiplying the capacitor's power-frequency reactance X_c with the instantaneous value of the current a quarter cycle earlier, $I\left(-\frac{1}{4}T\right)$. Therefore, the capacitor voltage estimation may be started after at least a quarter cycle of current samples is available. This is based on the assumption of steady-state sinusoidal conditions. This is shown in the start step in figure 5. Here, there are 200 samples per cycle, so 50 samples represent a quarter of a cycle. After initialization, the capacitor's voltage V_c for each subsequent sample is estimated by numerical integration of the capacitor's current as shown in equation 2, where dt is the sample interval.

$$V_c[i] = V_c[i-1] + \frac{dt}{C}\left(I[i-1] - I_{mov}[i-1]\right) \quad (2)$$

The capacitor's current is estimated as the difference between the measured current I into the bank and the estimated current I_{mov} bypassing the capacitor through the MOV. In non-fault conditions I_{mov} is practically zero. In fault conditions, if V_c reaches the MOV threshold V_{th}, then I_{mov} is found as a function of V_c from the MOV characteristic base 4th-order polynomial interpolation of figure 4 *b*.

Results for the presented method are shown in figure 6 and figure 7. The 'measured' voltage is from a direct

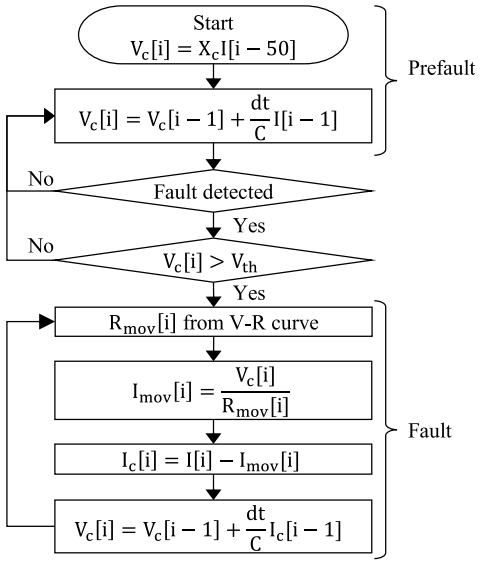

FIGURE 5. Process of capacitor voltage estimation; with 10 kHz sampling rate, 50 samples represent a quarter of a cycle.

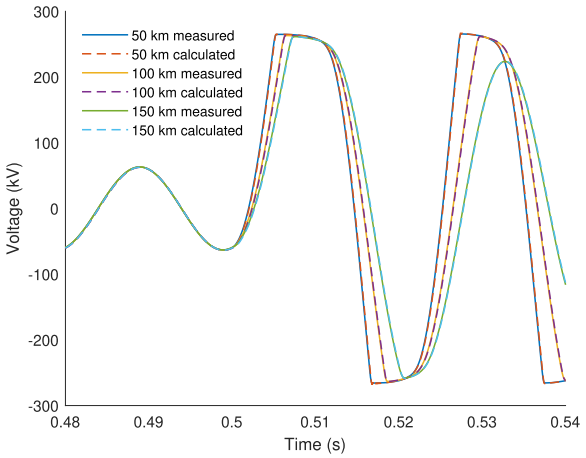

FIGURE 6. Capacitor voltage estimation compared to measured value for AG faults at 50 km, 100 km and 150 km, with 50% compensation.

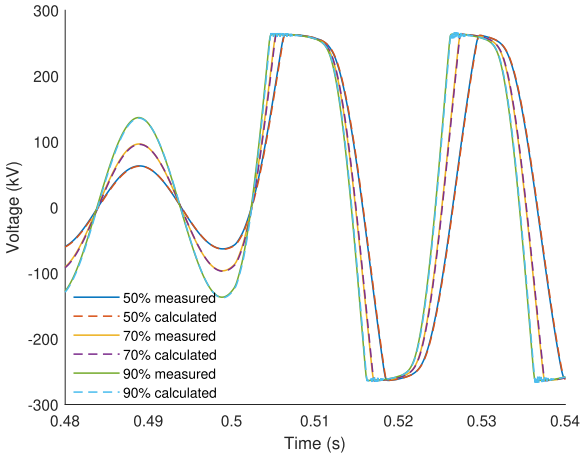

FIGURE 7. Capacitor voltage estimation compared to measured value for AG faults at 100 km, with 50%, 70% and 90% compensation.

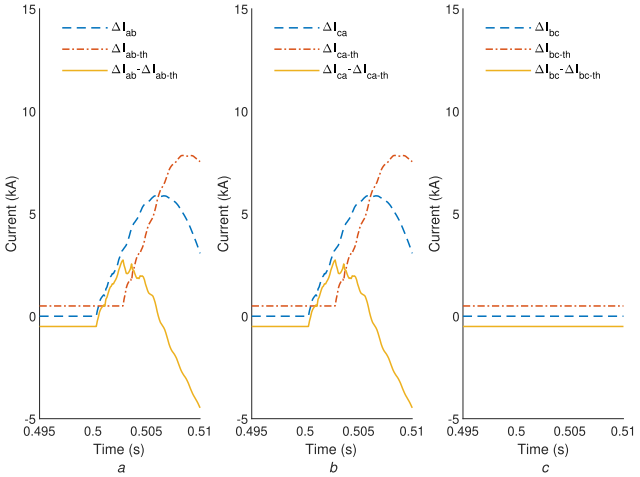

FIGURE 8. Fault detection for AG fault Δphase-phase currents a) ΔI_{ab} b) ΔI_{ca} and c) ΔI_{bc}.

measurement of the voltage across the capacitor in the PSCAD simulation. The estimated voltage is from the method described above. Figure 6 compares the estimated and measured values of capacitor voltage for different fault positions along the line, at 50% compensation level. Figure 7 does similarly for different compensation levels, with the fault position fixed at halfway along the line. In all these cases the measured and estimated values are seen to be very close.

B. FAULT DETECTION

The fault detection is based on a method presented in [22], using absolute value of incremental phase-to-phase current ($\Delta I_{\text{ph-ph}}$) and an adaptive threshold (ΔI_{th}). A fault is considered to exist if $\Delta I_{\text{ph-ph}} > \Delta I_{\text{th}}$. The ΔI_{th} is calculated as shown in equation 3, in which A and K are constants, I_N is the nominal current value, t is time and t_{D} is a delay.

$$\Delta I_{\text{th}} = A \left|\Delta I_{\text{ph-ph}}(t - t_{\text{D}})\right| + K I_N \tag{3}$$

This helps to restrict fault-detection to sharp changes in $\Delta I_{\text{ph-ph}}$ caused by faults, rather than slow-changing power system conditions such as power swings; the balance can be controlled by modifying the delay t_{D}. This method has been shown to work well with fault detection during power swings in [22], [27]. An example of fault detection is shown in figure 8 for an AG fault. The three subplots show the three phase-phase loop currents $\Delta I_{\text{ph-ph}}$ along with ΔI_{th} and their difference. The difference $\Delta I_{\text{ph-ph}} - \Delta I_{\text{th}}$ in subplots a and b crosses zero, indicating a fault; in subplot c which involves only the healthy phases B and C, the no-fault condition is detected.

C. PHASE SELECTION

Fault detection is followed by the selection of the faulty phase or phases. There are many ways to accomplish this. A method

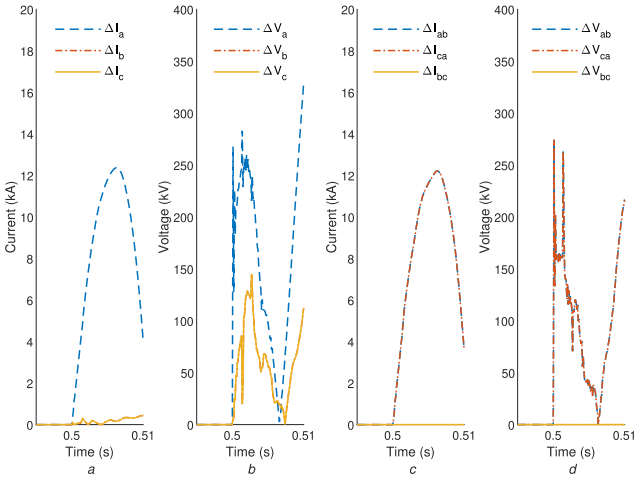

FIGURE 9. Phase selection for a AG fault a) Δ phase current b) Δ phase voltage c) Δ phase-phase current and d) Δ phase-phase voltage.

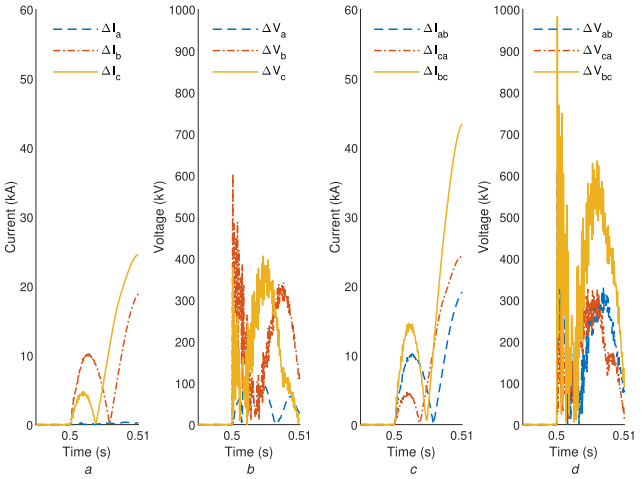

FIGURE 10. Phase selection for a BCG fault a) Δ phase current b) Δ phase voltage c) Δ phase-phase current and d) Δ phase-phase voltage.

with incremental voltage and current has been chosen here. The basis is that the incremental quantities in a faulted phase would be high and in a healthy phase would be close to zero. Absolute values are used in all the comparisons. For single-phase to ground faults,

- ΔI_{ph} of the faulty phase is high
- ΔV_{ph} of the faulty phase is high
- $\Delta I_{\text{ph-ph}}$ of healthy phases is close to zero
- $\Delta V_{\text{ph-ph}}$ of healthy phases is close to zero

Figure 9 shows the phase selection logic for a single-phase fault. This example is an AG fault, so ΔI_a and ΔV_a are high as shown in subplots *a* and *b*. Moreover, ΔI_{bc} and ΔV_{bc} are close to zero as shown in subplots *c* and *d*.

For phase-phase and phase-phase-ground faults,

- ΔI_{ph} of the faulty phases are high
- ΔV_{ph} of the faulty phases are high
- $\Delta I_{\text{ph-ph}}$ of faulty-faulty phases is higher than healthy-faulty phases
- $\Delta V_{\text{ph-ph}}$ of faulty-faulty phases is higher than healthy-faulty phases

Figure 10 shows the phase selection logic for a multi-phase fault. A BCG fault is used, so currents ΔI_b and ΔI_c are high as shown in subplot *a*. Also, voltages ΔI_a and ΔI_a are high as shown in subplot *b*. Then, ΔI_{bc} is higher than ΔI_{ab} and ΔI_{ca} as shown in subplot *c*. Finally, ΔV_{bc} is higher than ΔV_{ab} and ΔV_{ca} as shown in subplot *d*.

D. DIRECTIONAL DISCRIMINATION

Determining fault direction is a crucial part of the protection of series compensated lines, as voltage and current inversion pose challenges for phasor-based distance protection [8]. In transmission lines, fault direction can be determined by looking at the delta voltage and delta current as shown in [28]. In series compensated lines, to increase security, fault direction can be determined using delta voltage and the delta voltage drop across the line [29]. For a fault in the forward direction, the delta voltage and the delta voltage drop over the line have opposite polarity. For reverse fault, the delta voltage and delta voltage drop have the same polarity. It is important to calculate the delta voltage drop correctly, using the delta current and an impedance in differential form, $RI + L\frac{dI}{dt}$.

To demonstrate the directional discrimination, delta voltage (ΔV) and delta voltage drop (ΔIZ) over the line for all phases is shown for an ABCG fault in figure 11. The delta voltage and voltage drop for a phase always have opposite polarities for forward faults; this is also observed at zero crossings of these quantities.

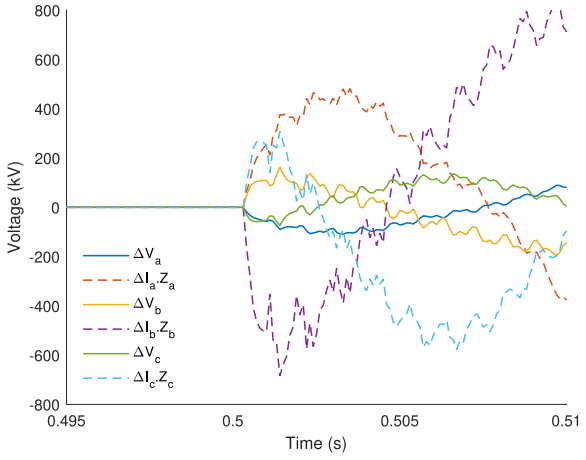

FIGURE 11. Directional discrimination for an ABCG fault.

E. DISTANCE ESTIMATION

Fault distance estimation is based on the difference between the absolute values of the voltage change due to the fault, V_{fault}, and the estimated pre-fault voltage V_{ref} at the end of the protected zone. V_{ref} is calculated from the pre-fault voltage, capacitor voltage and voltage drop over the line. V_{fault} is calculated from the fault delta voltage, the delta of capacitor

voltage and the delta of the voltage drop over the line and dependent on the fault type. A bolted fault would cause the voltage to reach close to zero at the fault point, so V_{ref} and V_{fault} are equal and opposite for bolted faults at the end of the protected zone. For faults inside the protected zone, V_{fault} is larger than V_{ref}.

The running (cumulative) sum of $V_{\text{fault}} - V_{\text{ref}}$ is an increasingly positive number for faults inside the protected zone, but close to zero or negative for faults outside the protected zone. This is demonstrated in figure 12. Subplot *a* compares V_{fault} for an AG fault at different positions along the line, and also the V_{ref} corresponding to 160 km, i.e. a protected zone of 80% of the 200 km line. It is seen that V_{fault} at 160 km km is close to the V_{ref}. Subplot *b* shows the running sum of $V_{\text{fault}} - V_{\text{ref}}$ for the same faults, along with a positive threshold for increased security. This threshold is useful for dealing with transients right after the fault; it can be modified to balance security and speed of operation.

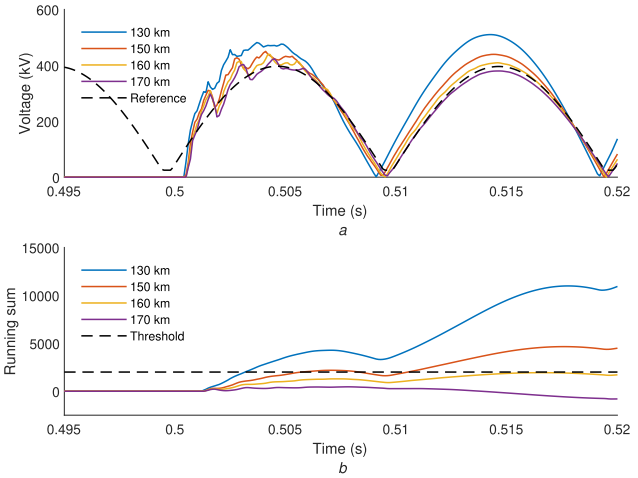

FIGURE 12. Distance estimation for an AG fault at various distances: a) estimated fault voltage and reference voltage at fault point; b) cumulative voltage difference between estimated and reference voltages.

III. TEST DESCRIPTION

For more extensive testing of the method, a large number of test cases were simulated in PSCAD [26]. The simulated model is similar to figure 2, with a 500 kV, 200 km transmission line. The details of the line parameters used in the simulation model are given in table 1. The different parameter values used in generating the test cases are shown in table 2. The fault inception angle is varied by taking 0° and 90° relative to phase-A voltage. As faults on phases B and C are also studied, this gives good coverage of fault inception angles when considered relative to faulted-phase voltage: for example, a BG fault incepted at 0° relative to phase-A voltage corresponds to 120° for the faulted (B) phase. Two values of source impedance ratio (SIR) are used: 0.20 and 0.35. This range was chosen because series capacitors are usually used in long lines, and long lines are defined with SIR < 0.50 [30].

TABLE 1. Transmission line parameters.

Parameter	Value
Line length	200 km
Conductor	
Type	Chukar
Geometric mean radius	20.345 mm
DC resistance	0.0318 Ω/km
Strands	84
Strand radius	1.8491 mm
Relative permeability	1.0
Sag	12 m
Height	22 m
Sub-conductor	2
Sub-conductor spacing	0.4572 m
Ground wire	
Number	2
Radius	5.5245 mm
DC resistance	2.8645 Ω/km
Relative permeability	1.0
Sag	10 m
Height	10 m
Impedance	
Positive sequence	$0.018 + j0.339$ Ω/km
Zero sequence	$0.266 + j1.017$ Ω/km
Compensation	
50%	≈ 94 μF
60%	≈ 78 μF
70%	≈ 67 μF

TABLE 2. Test cases considered.

Parameter	Value
Phase A inception angle (°)	0, 90
Source impedance ratio (SIR)	0.20, 0.35
Compensation level (%)	50, 60, 70
Resistance (Ω)	0.10, 10, 20, 30
Location (%)	−5, 5, 25, 50, 62.5, 75 77.5, 80, 82.5, 85, 90, 95
Fault type	NF, AG, BG, CG ABG, CAG, BCG, ABCG AB, CA, BC, ABC

Compensation level k is defined as in equation 4 by the proportion of line inductive reactance X_{L} compensated by the capacitor's reactance X_{C}. Three levels of compensation are used.

$$k = \frac{X_{\text{C}}}{X_{\text{L}}} \tag{4}$$

Four different fault resistances are used: 0.01 Ω for bolted faults, then 10 Ω, 20 Ω and 30 Ω to study the effect of fault resistance. These values are reasonable for the selected voltage level and both single and multi-phase faults [31]. The fault location is varied from a close reverse fault (−5%) up to well beyond the protected zone (95%). The percentage shows the position of the fault from the measuring point, relative to line length. The protected zone was set to extend to 80%, and fault cases are tested at several distances close to this 80% boundary. The reverse faults were included to test the effectiveness of the directional discrimination logic. All the

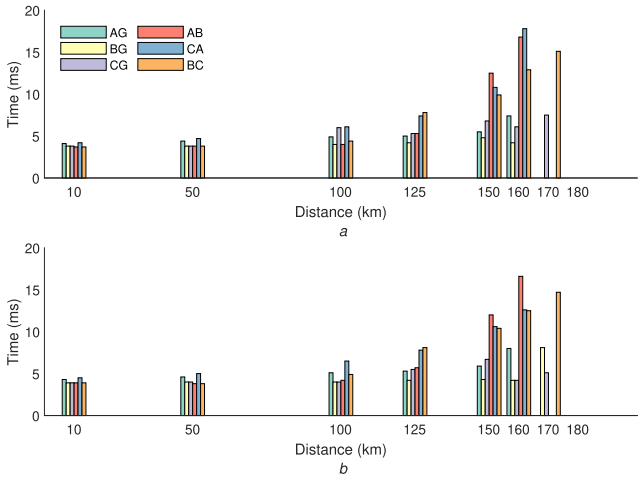

FIGURE 13. Decision time for 0° inception angle, 50% compensation and 0.10 Ω fault resistance with SIR a) 0.20 and b) 0.35.

fault types available in PSCAD are tested, including no-fault (NF) conditions.

Combining all the factors shown in table 2, a total of 6912 test cases were produced. PSCAD provides an automation library (AL) developed in Python to interface with PSCAD. It is available for all PSCAD users and can be used to automate simulations. Simulation and saving of results were automated with a Python script based on the PSCAD AL, with some manual checking of results. PSCAD provides detailed documentation of the AL that can be used to build a suitable script for simplifying running lots of simulations with various parameters. Each simulation was run for 1 s with a 10 kHz sampling frequency. All the simulation output data along with a PSCAD model and example python script are published as open data [32]. An implementation of the proposed method in Matlab was used to read the simulation output and report at what time any trip decision was made for each case.

IV. RESULTS AND DISCUSSION

This section presents results from the tests based on table 2. The decision time shown in figure 13 to figure 17 is the time required by the method shown in figure 1 to detect the fault after fault inception. It includes fault detection, phase selection, directional discrimination and distance estimation.

The algorithm decision times are not intended for a detailed comparison, but only as an indication of the potential of the proposed method and the approximate sensitivity to the studied set of parameters. In a relay implementation, these times may vary with chosen sampling rate, processor type or security requirements. Additionally, trip times and reach are affected by various thresholds in the code, which can be increased or decreased to modify the sensitivity, speed and security and can be treated as some sort of relay settings.

In general, this time domain based method shows a faster trip time compared to phasor based methods. The faults at short distances (e.g. 10 km, 50 km) after the capacitor would cause current and/or voltage inversion in a phasor based method. However, the fast trip times over a wide range of settings ensure that these phenomena do not affect the performance of incremental quantity protection. A general trend observed in power system protection literature is the increasing higher demand for faster trip times for protection relays [33], [34]. However, it is also important to notice that the trip time for the relay is only a small part of the total fault clearing time [35], when used in systems with conventional high-voltage circuit breakers rather than high-speed current-limiting breakers that are proposed for DC systems and special AC applications. Nonetheless, the proposed method shows good potential for series compensated line protection, with decision times under 1/2 cycle in most cases.

In figures 13-16 the impact on the effectiveness of the proposed method is shown for four parameters: SIR, inception angle, compensation level and fault resistance. In each figure, one parameter is varied while the other three are kept constant. As it is difficult to show results from all of the 6912 tests, only a selection of fault distances and fault types are shown in the figures. In each case, trip times for fault types AG, BG, CG, AB, CA and BC are shown as different coloured bars, at distances 10, 50, 100, 125, 150, 160, 170 and 180 km shown on the horizontal axis. The absence of a visible bar means the method did not issue a trip signal. Recall that the protected zone is set to reach up to 160 km (80%) of the line length.

Figure 13 shows the influence of SIR, with 0° inception angle (relative to phase-A voltage), 50% compensation and 0.10 Ω fault resistance. Subplots *a* and *b* show trip times for SIR 0.20 and 0.35. The difference in decision time is not significant between these two SIR values. Differences are mainly seen around the critical 160 km distance. Longer decision times are observed with distant faults. A few over-reaches are seen at the 170 km fault distance; this can be explained by the high current from the low fault resistance, and different fault inception angles from phases B and C.

Figure 14 shows the influence of different fault inception angles, with 0.20 SIR, 50% compensation, and 0.10 Ω fault resistance. Subplots *a* and *b* show results for fault inception angles 0° and 90°. Inception angles are relative to phase-A voltage as described earlier, leading to different combinations of fault angles for phases B and C. Again there is not a significant difference between the subplots. A few over-reaching cases are observed for different fault types in both subplots.

Figure 15 shows the influence of different compensation levels, with 0.20 SIR, 0° inception angle and 0.10 Ω fault resistance. The three subplots show test cases for 50%, 60% and 70% compensation. The decision times in the three subplots again show no significant differences. As usual, there are some over-reach cases in all three subplots.

Figure 16 shows the influence of fault resistance, with 50% compensation, 0.20 SIR and 0° inception angle. The subplots show the test cases with fault resistances 0.10 Ω, 10 Ω and 20 Ω. The fault resistance is seen to have a considerable impact on the operation of the proposed method. As the fault resistance increases, more under-reach is observed. Higher fault resistances cause no trip for faults just inside the reach.

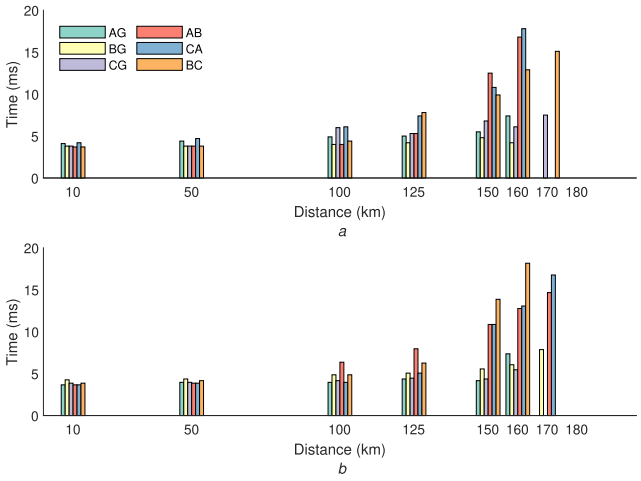

FIGURE 14. Decision time for 0.20 SIR, 50% compensation and 0.10 Ω fault resistance with fault inception angles a) 0° and b) 90°.

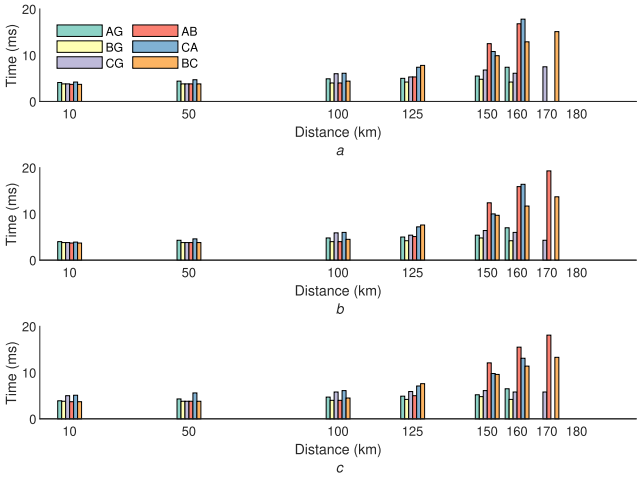

FIGURE 15. Decision time for 0.20 SIR, 0° inception angle and 0.10 Ω fault resistance with compensation levels a) 50% b) 60% and c) 70%.

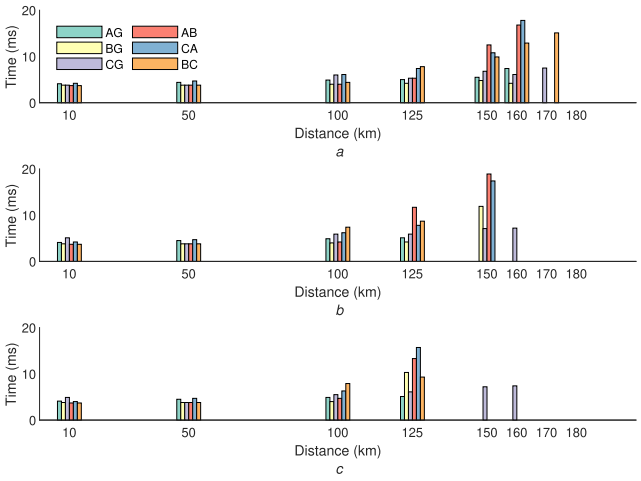

FIGURE 16. Decision time for 0.20 SIR, 0° inception angle and 50% compensation with fault resistances a) 0.10 Ω b) 10 Ω and c) 20 Ω.

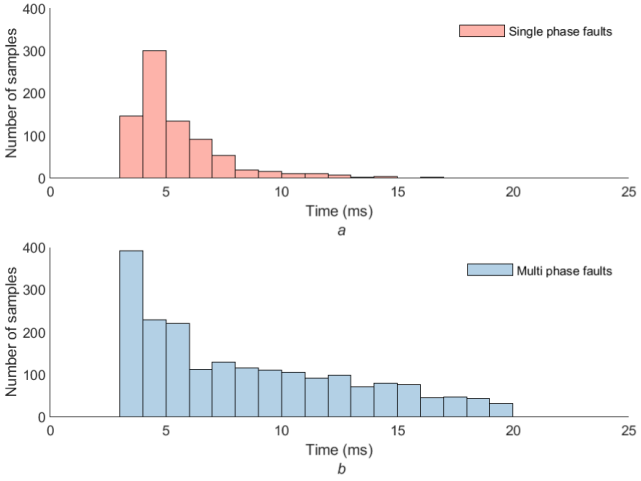

FIGURE 17. Histogram of decision times for different test cases a) single phase faults b) multi phase faults.

This is due to the assumption mentioned in subsection II-E, that the voltage at the fault point is close to zero. The reference voltage estimated for a fault at the reach point is based on this assumption. However, for higher fault resistance, the voltage drop in the fault point is higher, leading to lower voltage estimation at the fault point and reduced reach. The method can be optimized to work with higher fault resistances, but then there will be more over-reach when low fault resistances are encountered. In an actual system, the method can be tuned to work appropriately with the most likely fault resistance, and then some level of over/under reach will be observed at lower/higher fault resistances.

Finally, in figure 17, decision times for all test cases are presented in a histogram. A finite decision time indicates fault detection and operation and no decision time indicates no operation by the relay. It gives an indication of the number of test cases with different decision times. Subplot *a* shows times for the single-phase faults. Subplot *b* shows the times for the faults involving multiple phases. In subplot *a*, there are 806 decision times out of a possible 1008 cases. In subplot *b*, there are 2019 decision times out of a possible 2688 cases. The lower number of decisions is due to reduced reach in high resistance faults close to the zone reach. In the test cases, most of the fault distances are close to the zone reach, so under-reaching cases are seen more in the histogram. The decision time shows a promising distribution in both subplots. In single-phase faults, most faults are detected within 1/4 of a cycle or lower. Most faults involving multiple phases are also detected within 1/4 of a cycle or lower, but the distribution is more spread out as multiple voltages and currents need to be considered. It also needs to be considered that most test cases concern faults closer to the zone reach rather than to the relay; figures 13 to 16 show that more distant faults result in a longer time to operate, so those cases skew the distribution to higher decision times. As the proposed method works with local measurement only, it can be compared with phasor based distance protection that also works with this type of measurement. It is well known [2], [3] that distance relays experience delays and the directional problem with series compensation. The operation time can reach to few

cycles. As seen from the test cases, the proposed method works in a much shorter time frame. It does not suffer from delay and directional problems similar to the phasor based distance relay.

V. CONCLUSION

In this paper time-domain based incremental quantity protection is shown to work for the protection of series compensated lines. The results are positive based on the fact that the given method is simple and the verification has confirmed the method. However, it needs to be noted that incremental quantity solution based on the time-domain signal measurement is only strictly appropriate to a linear system with fixed source values. If significant nonlinearity is expected during the timescale of the fault, for example, due to inverter-interfaced sources, the performance of the algorithm should be further evaluated. Additionally, some areas can be looked into in further work. This paper demonstrates the proposed method on a series capacitor located in the line terminal with a current and voltage transformer. This essentially means that the current through the series capacitor is the same as the current-transformer measurement. The capacitor voltage estimation is based on current through the capacitor. Therefore, this method will need to be modified for capacitors in the middle of the line. Additionally, as the method is based on voltage drop, a high resistance fault is shown to cause an under-reach situation in the distance measurement. The distance measurement will not operate with faults with higher resistances. Another issue is that the capacitor voltage and current are assumed to be in a steady state when initializing the process. There are also possibilities to improve the numeric stability of the integration.

The proposed method works with local measurement only. In future, it can be evaluated in the presence of communication between the protected line terminals. The security of this method will be increased in the presence of communication with the remote bus. As some transmission system operators have communication channels in their transmission lines for differential protection, this may be an interesting area for future development tasks.

The proposed method has been tested with different test cases and performs well with varied SIR, capacitance, fault inception angle etc. The different test cases are also published as open source for other researchers interested in series compensated lines. The time for decision is also well within desired values expected of protection relays. Although there is room for improvement, this paper can work as a proof of concept for the application of incremental quantity protection for series compensated transmission lines.

REFERENCES

[1] O. Ojo, "Optimal series capacitor compensation of high voltage transmission lines," in *Proc. 23th Southeastern Symp. Syst. Theory*, Mar. 1991, pp. 550–554.

[2] *Protection, Control and Monitoring of Series Compensated Networks*, CIGRE, Paris, France, 2010.

[3] *Challenges With Series Compensation Applications in Power Systems When Overcompensating Lines*, CIGRE, Paris, France, 2021.

[4] M. T. Hoq, J. Wang, and N. Taylor, "Impact of high levels of series compensation on line distance protection," in *Proc. 15th Int. Conf. Develop. Power Syst. Protection*, Liverpool, U.K., 2020, pp. 1–7.

[5] E. Bakie, C. Westhoff, N. Fischer, and J. Bell, "Voltage and current inversion challenges when protecting series-compensated lines—A case study," in *Proc. 69th Annu. Conf. Protective Relay Eng.*, College Station, TX, USA, Apr. 2016, pp. 1–14. [Online]. Available: http://ieeexplore.ieee.org/document/7914925/

[6] M. T. Hoq, J. Wang, and N. Taylor, "The Impact of current inversion on line protection in high voltage transmission lines with series compensation," in *Proc. Conf. Energy, Power Syst. Power Ind. Electron.*, Narvik, Norway, 2019, pp. 1–8.

[7] B. Vyas, R. P. Maheshwari, and B. Das, "Protection of series compensated transmission line: Issues and state of art," *Electr. Power Syst. Res.*, vol. 107, pp. 93–108, Feb. 2014. [Online]. Available: https://linkinghub.elsevier.com/retrieve/pii/S0378779613002587

[8] M. T. Hoq, J. Wang, and N. Taylor, "Review of recent developments in distance protection of series capacitor compensated lines," *Electr. Power Syst. Res.*, vol. 190, Jan. 2021, Art. no. 106831.

[9] F. Ghassemi, J. Goodarzi, and A. T. Johns, "Method to improve digital distance relay impedance measurement when used in series compensated lines protected by a metal oxide varistor," *IEE Proc. Gener., Transmiss. Distrib.*, vol. 145, no. 4, pp. 403–408, Jul. 1998.

[10] D. L. Goldsworthy, "A linearized model for mov-protected series capacitors," *IEEE Trans. Power Syst.*, vol. PS-2, no. 4, pp. 953–957, Nov. 1987.

[11] M. M. Saha, B. Kasztenny, E. Rosolowski, and J. Izykowski, "First zone algorithm for protection of series compensated lines," *IEEE Trans. Power Del.*, vol. 16, no. 2, pp. 200–207, Apr. 2001.

[12] E. Rosolowski, J. Izykowski, P. Pierz, M. Fulczyk, P. Balcerek, and M. M. Saha, "High voltage series-compensated transmission line—Evaluation of new distance protection," in *Proc. Int. Conf. High Voltage Eng. Appl.*, Oct. 2010, pp. 513–516.

[13] U. J. Shenoy, P. Sandeep, and S. Srivastava, "Impact of MOV models on asymmetrical fault current calculations in fixed series compensated lines," in *Proc. Asia-Pacific Power Energy Eng. Conf. (APPEEC)*, Nov. 2017, pp. 1–6.

[14] M. M. Saha, E. Rosolowski, J. Izykowski, and P. Pierz, "Evaluation of relaying impedance algorithms for series-compensated line," *Electr. Power Syst. Res.*, vol. 138, pp. 106–112, Sep. 2016.

[15] A. C. C. Q. A. Figueiredo, W. L. A. Neves, and D. Fernandes, "Evaluation of phasor estimation methods for transmission lines with capacitive series compensation," in *Proc. Simposio Brasileiro Sistemas Eletricos*, May 2018, pp. 1–6.

[16] M. Biswal, B. B. Pati, and A. K. Pradhan, "Adaptive distance relay setting for series compensated line," *Int. J. Electr. Power Energy Syst.*, vol. 52, pp. 198–206, Nov. 2013.

[17] M. M. Saha and T. Einarsson, "A new adaptive high speed distance protection scheme for power transmission lines," in *Proc. 13th Int. Conf. Develop. Power Syst. Protection (DPSP)*, Mar. 2016, pp. 1–6.

[18] N. Davydova, D. Shchetinin, and G. Hug, "Optimization of first zone boundary of adaptive distance protection for flexible transmission lines," in *Proc. Conf. Power Syst. Comput. Conf.*, Jun. 2018, pp. 1–7.

[19] M. T. Hoq and N. Taylor, "Distance protection of series capacitor compensated lines: Practical considerations, industrial status and development," *Electricity*, vol. 2, no. 2, pp. 168–186, May 2021. [Online]. Available: https://www.mdpi.com/2673-4826/2/2/11

[20] D. Danylov, "Evaluation of symmetrical components theory in power systems with renewable sources," M.S. thesis, Dept. Elect. Eng. Comput. Sci., KTH Royal Inst. Technol., Stockholm, Sweden, 2021.

[21] E. O. Schweitzer, B. Kasztenny, A. Guzman, V. Skendzic, and M. V. Mynam, "Speed of line protection—Can we break free of phasor limitations?" in *Proc. 68th Annu. Conf. Protective Relay Eng.*, College Station, TX, USA, Mar. 2015, pp. 448–461. [Online]. Available: http://ieeexplore.ieee.org/document/7102184/

[22] J. Blumschein, C. Dzienis, and M. Kereit, "Directional comparison based on high-speed-distance protection using delta quantities," Siemens AG, Infrastruct. Cities Sector, Munich, Germany, Tech. Rep., 2014.

[23] E. O. Schweitzer, B. Kasztenny, and M. V. Mynam, "Performance of time-domain line protection elements on real-world faults," in *Proc. 69th Annu. Conf. Protective Relay Eng.*, College Station, TX, USA, Apr. 2016, pp. 1–17. [Online]. Available: http://ieeexplore.ieee.org/document/7914904/

[24] C. Dzienis, M. Kereit, J. Blumschein, and M. Claus, "An experimental analysis of high-speed-distance protection," in *Proc. Mod. Electr. Power Syst.*, Wroclaw, Poland, 2010, p. 8.
[25] C. Dzienis, M. Kereit, and J. Blumschein, "Analysis of high-speed-distance protection," in *Proc. Int. Conf. Adv. Power Syst. Automat. Protection*, Beijing, China, Oct. 2011, pp. 1330–1336. [Online]. Available: http://ieeexplore.ieee.org/document/6180585/
[26] Manitoba Hydro International. *PSCAD*. Version 4.64. [Online]. Available: https://www.pscad.com/
[27] S. H. Hasan Kazmi, J. Wang, and Y. Li, "Comparison of high-speed transient-based pilot directional protection algorithms for distribution grids," in *Proc. IEEE Innov. Smart Grid Conf. Eur.*, Sarajevo, Bosnia, Oct. 2018, pp. 1–5. [Online]. Available: https://ieeexplore.ieee.org/document/8571647/
[28] J. Wang, Y. Li, P. Cost, and S. Zubic, "A novel pilot protection for transmission lines based on full travelling wave signal polarities," in *Proc. 15th Int. Conf. Develop. Power Syst. Protection (DPSP)*, Jan. 2020, pp. 1–6. [Online]. Available: https://digital-library.theiet.org/content/conferences/10.1049/cp.2020.
[29] M. Kockott, S. Zubic, Z. Liu, H. Jernberg, T. Roseburg, and W. Rees, "A POTT scheme, using transient directional elements, for a complex 525 kV transmission corridor comprising long, heavily loaded and heavily series compensated parallel lines," in *Proc. Western Protective Relay Conf.*, Atlanta, GA, USA, 2019, p. 10.
[30] M. J. Thompson and A. Somani, "A tutorial on calculating source impedance ratios for determining line length," in *Proc. 68th Annu. Conf. Protective Relay Eng.*, College Station, TX, USA, Mar. 2015, pp. 833–841. [Online]. Available: http://ieeexplore.ieee.org/document/7102207/
[31] V. D. Andrade and E. Sorrentino, "Typical expected values of the fault resistance in power systems," in *Proc. Transmiss. Distrib. Conf. Expo., Latin Amer.*, Nov. 2010, pp. 602–609.
[32] M. T. Hoq. (Jun. 2021). *Fault Test Cases for Series Compensated Transmission Lines*. [Online]. Available: https://zenodo.org/record/5113208#.YPgORugzZaQ
[33] J. Mooney, G. Benmouyal, N. Fischer, and B. Kasztenny, "Transmission line protection system for increasing power system requirements," in *Proc. Mod. Electr. Power Syst.*, Sep. 2010, pp. 1–11.
[34] B. P. Administration, "Technical requirements for interconnection to the BPA transmission grid," BPA, Portland, OR, USA, Tech. Rep. STD-N-000001 REVISION 07 CN 01, 2016.
[35] S. Zubic, Z. Gajic, and D. Kralj, "Line protection operate time: How fast shall it be," *IEEE Access*, vol. 9, pp. 75608–75616, 2021.

MD. TANBHIR HOQ received the B.Sc. degree in electrical and electronic engineering from the Islamic University of Technology (IUT), Bangladesh, in 2011, and the EIT KIC InnoEnergy SENSE double M.Sc. degree from KU Leuven, Belgium, and KTH, Sweden, in 2014. He is currently pursuing the Ph.D. degree with KTH. From 2015 to 2017, he worked at the Swedish Power Industry for ABB Capacitors (Ludvika), ABB FACTS (Västerås), and FMTP Power AB (Stockholm) in several projects. In 2017, he returned to academia and worked as a Lecturer at the University of Asia Pacific (UAP), Bangladesh.

JIANPING WANG (Senior Member, IEEE) received the Ph.D. degree in Belgium, in 1993. In 1995, he joined ABB, and has worked with different roles, such as Research and Development Engineer, Application Specialist, a System Engineer, the Technical Market Manager, the Technical Director, and a Senior Principal Scientist with ABB and Hitachi Energy. He is currently working as a Senior Principal Scientist at the Research Center of Hitachi Energy, Västerås, Sweden. He has published more than 50 papers in the related international conferences and journals. His main research interest includes power system protection.

NATHANIEL TAYLOR received the M.Eng. degree in electrical and electronic engineering from Imperial College London, in 2001, and the Ph.D. degree in high voltage engineering from KTH, in 2010. He is currently an Associate Professor in electrical engineering at KTH, working with power system protection, safety, and monitoring. His work includes aspects of all levels of the power systems, and involves utilities and manufacturers. He is also extensively involved in teaching electric fundamentals and power engineering for students from B.Sc. level upwards.